

Boise State University

ScholarWorks

Materials Science and Engineering Faculty
Publications and Presentations

Micron School for Materials Science and
Engineering

2021

Influence of the InAs Coverage on the Performance of Submonolayer-Quantum-Dot Infrared Photodetectors Grown with a (2×4) Surface Reconstruction

Ahmad Alzeidan
University of Sao Paulo

Tiago F. De Cantalice
University of Sao Paulo

Kevin D. Vallejo
Boise State University

Paul J. Simmonds
Boise State University

Alain A. Quivy
University of Sao Paulo

Influence of the InAs coverage on the performance of submonolayer-quantum-dot infrared photodetectors grown with a (2×4) surface reconstruction.

Ahmad Alzeidan
Institute of Physics,
University of Sao Paulo
Sao Paulo, Brazil
Email: alzeidan@if.usp.br

Tiago F. de Cantalice
Institute of Physics
University of Sao Paulo
Sao Paulo, Brazil
Email: cantalice.tiagof@gmail.com

Kevin D. Vallejo
Micron School of Materials Science
and Engineering
Boise State University.
Boise, USA
Email: kevinvallejo@u.boisestate.edu

Paul J. Simmonds
Micron School of Materials Science
and Engineering
Boise State University
Boise, USA
Email: paulsimmonds@boisestate.edu

Alain A. Quivy
Institute of Physics
University of Sao Paulo
Sao Paulo, Brazil
Email: aquivy@if.usp.br

Abstract—Two infrared photodetectors based on submonolayer quantum dots, having a different InAs coverage of 35% and 50% of a monolayer, were grown, processed and tested. The detector with the larger coverage yielded a specific detectivity of $1.13 \times 10^{11} \text{ cm Hz}^{1/2} \text{ W}^{-1}$ at 12K, which is among the highest values reported in the literature for that kind of device.

Keywords—quantum dot, submonolayer, infrared photodetector, molecular beam epitaxy, surface reconstruction, segregation.

I. INTRODUCTION

Over the past few decades, self-assembled quantum dots (QDs) have shown to be of great interest for the manufacture of infrared photodetectors [1, 2]. When compared to the same devices based on quantum wells, the advantages of quantum-dot infrared photodetectors (QDIPs) originate from their sensitivity to normal-incidence radiation, three-dimensional confinement of carriers, and reduced dark current and noise [3]. Usually, QDs are fabricated using the Stranski-Krastanov growth mode [4], which consists of depositing a thin layer of material on top of a substrate having a smaller lattice parameter. Above a critical thickness, the strained epitaxial layer will partially relax and form a homogeneous distribution of small islands all over the surface. In the specific case of the InAs/GaAs system, small InAs islands form beyond a critical thickness of 1.7 monolayers (MLs) and behave as quantum dots due to the smaller gap of their material when compared to GaAs. Such Stranski-Krastanov quantum dots (SK-QDs) form spontaneously, have a density in the low to medium 10^{10} cm^{-2} range, have a base and height around 20 nm and 7 nm, respectively, are surrounded by a thin InGaAs layer (called the wetting layer), and have a size that is difficult to control (a direct consequence of the self-assembly process).

An alternative method to obtain QDs in a much more controllable way, with a smaller size and without a wetting layer, is the submonolayer technique [5]. InAs/GaAs

submonolayer quantum dots (SML-QDs) can be obtained by depositing a fraction of a monolayer (ML) of InAs material—generally between 0.35 ML and 0.50 ML [6–8]—in order to nucleate a high density of small two-dimensional (2D) islands on the GaAs substrate, and then covering these islands with a specific number of GaAs monolayers. By repeating this sequence as many times as necessary, the strain field—originating from the lattice mismatch between both materials—will contribute to align the small 2D islands of consecutive InAs submonolayers to form stacks that will behave as individual QDs [9].

As the growth of SML-QDs is more complex than that of conventional SK-QDs and involves more experimental parameters, its optimization is more difficult and is still under debate in the literature. For instance, almost all papers report growth conditions similar to the ones of conventional SK-QDs, together with a low substrate temperature and a high As flux that provides a c(4×4) reconstruction of the GaAs(001) surface prior to deposition [10–12]. However, it seems that a much lower As flux and a (2×4) surface reconstruction might be the only way to truly form 2D InAs islands on the GaAs(001) surface [13,14]. In addition, only a few reports exist concerning the optimization of their main growth parameters, such as the III-V flux ratio [9,15], growth rates [9], number of deposition cycles [7], InAs coverage [16], and the use of different materials or compositions [17].

In the present work, we used two different monolayer fractions of InAs material in the cyclic deposition in order to check their influence on the performance of SML-QDs-based infrared photodetectors (SML-QDIPs) grown in the presence of a (2×4) surface reconstruction.

II. EXPERIMENTAL DETAILS

The two SML-QDIPs (samples A and B) were grown on a semi-insulating GaAs(001) substrate by molecular beam epitaxy (MBE) using a valved As cracker in order to allow large changes of As₂ flux within a few seconds.

This study was financed in part by the Coordenação de Aperfeiçoamento de Pessoal de Nível Superior - Brasil (CAPES) - Finance Code 001 and by CNPq (grant 311687/2017-2).

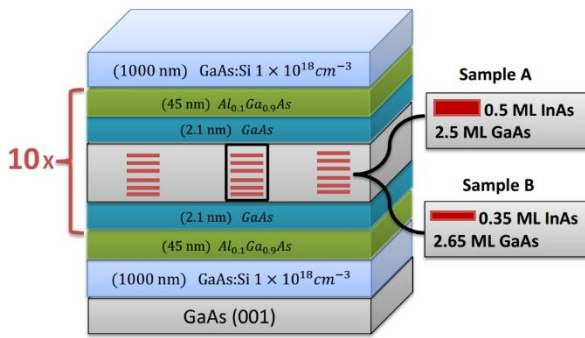


Fig. 1: Structure of the two SML-QDIPs with different InAs fractions. The black rectangle shows a single SML-QD formed by repeating six times the growth cycle.

After oxide removal and degassing of the epi-ready substrates at 615 °C for 5 minutes, two 1 μm -thick Si-doped GaAs layers ($n=1 \times 10^{18} \text{ cm}^{-3}$) were grown at 570 °C and acted as bottom and top contacts. Between them, the active region of the devices was formed by 10 layers of SML-QDs, each of them inserted inside an 8.5 nm-wide GaAs quantum well having 45 nm-thick $\text{Al}_{0.1}\text{Ga}_{0.9}\text{As}$ barriers (Fig. 1). Each SML-QD layer was built from the sequential deposition of InAs (deposited at 0.014 monolayer per second (ML/s)) followed by GaAs (deposited at 0.1 ML/s), and this sequence was repeated 6 times. In sample A, 0.5 ML of InAs was deposited and followed by 2.5 MLs of GaAs, while, in sample B, 0.35 ML of InAs was followed by 2.65 MLs of GaAs. Each thin GaAs layer was Si-doped at $2 \times 10^{18} \text{ cm}^{-3}$ in order to provide free carriers to the SML-QDs. The active region was grown at 490 °C, and the As_2 flux had to be considerably reduced (to 0.25 ML/s) to recover a (2×4) surface reconstruction [18] instead of the $c(4 \times 4)$ reconstruction usually obtained at such temperature. The rest of the sample was grown at 570 °C and with a much higher As_2 flux, equivalent to 1.75 ML/s. *In-situ* reflection high-energy electron diffraction (RHEED) was used to calibrate the growth rates of all the materials and to accurately determine the transition between the $c(4 \times 4)$ and (2×4) surface reconstructions as a function of the As flux and sample temperature.

Both samples were processed into $400 \times 400 \mu\text{m}^2$ photodetectors using standard optical lithography, wet etching, and electron-beam metallization (Ni, Ge, and Au). Rapid thermal annealing at 520 °C for 30 s was used to obtain good Ohmic contacts. Each device was wire-bonded to a chip carrier and then fixed on the cold finger of an optical cryostat operating between 12 and 300 K. Photocurrent, spectral response, dark current, and noise measurements were finally carried out to analyze their performance.

III. RESULTS AND DISCUSSION

The spectral response of the devices was obtained at 12 K using normal-incidence Fourier transform infrared (FTIR) spectroscopy and is reported in Fig. 2. It shows that the absorption of sample B is broader and redshifted ($\lambda = 12.2 \mu\text{m}$, $\Delta\lambda/\lambda \approx 0.17$) compared to sample A ($\lambda = 11.54 \mu\text{m}$, $\Delta\lambda/\lambda \approx 0.13$). In general, a low InAs coverage leads to narrower 2D islands, whose density increases with increasing amount of material. However, beyond a certain amount of material,

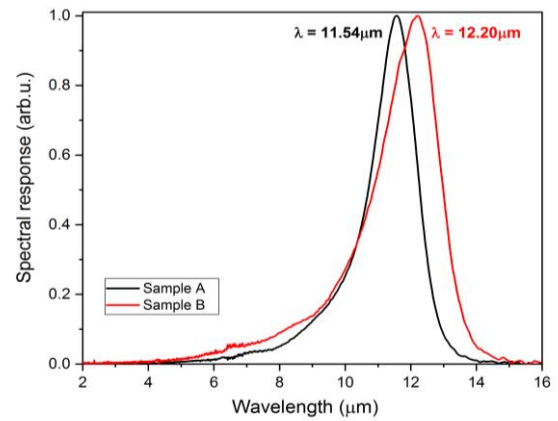


Fig. 2: Normalized spectral response as a function of wavelength at 12 K for a bias of -1.2 V.

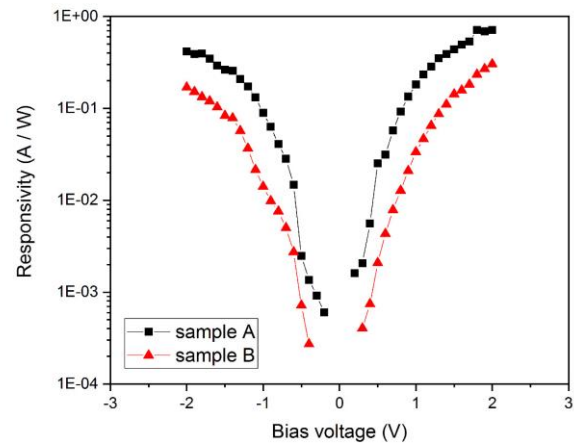


Fig. 3: Black-body responsivity as a function of bias at 12 K.

the density decreases as the small islands start to merge, yielding wider 2D islands. As sample A already has 50% of its surface covered by InAs material, we can expect it to have a lower density of larger 2D islands than sample B. The broader peak of sample B is therefore related to the narrower size of the SML-QDs, whose size fluctuations have a larger influence on the value of the ground-state energy, when compared to wider SML-QDs (quantum effects are stronger for smaller structures). The redshift can be attributed to the lower transition energy between the higher ground state of the narrower SML-QDs of sample B and the excited state of the QW that is close to the top of the $\text{Al}_{0.1}\text{Ga}_{0.9}\text{As}$ barrier.

The responsivity of both devices was calculated using the photocurrent measured in front of a calibrated blackbody set at 800 °C, and then dividing this value by the useful spectral power of the blackbody radiation reaching the devices. Fig. 3 shows that, for a given bias, the responsivity of sample A is typically four times higher than that of sample B. It means that sample A provides 4 times more output signal than sample B, under the same experimental conditions, despite the fact that it has a lower density of SML-QDs than sample B.

Then, the devices were covered with a copper shield in order to perform current-voltage (I-V) curves in the dark as well as noise measurements. As this shield was in thermal contact with the sample holder, it also acted as a cold shield.

Fig. 4a shows that the dark current of sample A is generally higher than that of sample B by one order of magnitude. This is also unexpected, as sample B has narrower SML-QDs and should therefore have a higher ground state than in sample A, as already pointed out in Fig. 2. Consequently, one might expect carriers to escape more easily from SML-QDs of sample B, leading to a higher dark current. To confirm this, I-V curves in the dark (dark current) were measured as a function of temperature, and an Arrhenius plot of the dark current at a fixed bias voltage (Fig. 4b) was used to calculate the activation energy, which can be obtained from the slope of the linear section of the data above 50 K. One can see that the activation energy of sample A (61.4 meV) is actually slightly smaller than the one of sample B (73.2 meV), what explains the lower dark current of sample B. To understand this phenomenon, one must remember that, in this kind of measurement, the activation energy is the difference between the Fermi level of the system and the top of the $\text{Al}_{0.1}\text{Ga}_{0.9}\text{As}$ barrier of the QW (continuum), and not between the ground state of the SML-QDs and the top of the barrier, as is often assumed [19]. Since the only difference between both samples was the InAs coverage—the doping was not altered—and sample B is supposed to have more SML-QDs than sample A, these SML-QDs are not ideally doped (2 electrons in the ground state), and their Fermi energy is naturally lower than in sample A where all the SML-QDs are supposedly fully doped (the doping was originally adjusted for the density of SML-QDs of sample A). In addition, it is well known that the InAs/GaAs system is strained, and each QD introduces a certain density of structural defects that are potentially able to trap carriers. As a consequence, sample B must have a lower density of free carriers originating from the dopant atoms, which also contributes to lower the Fermi energy of that sample.

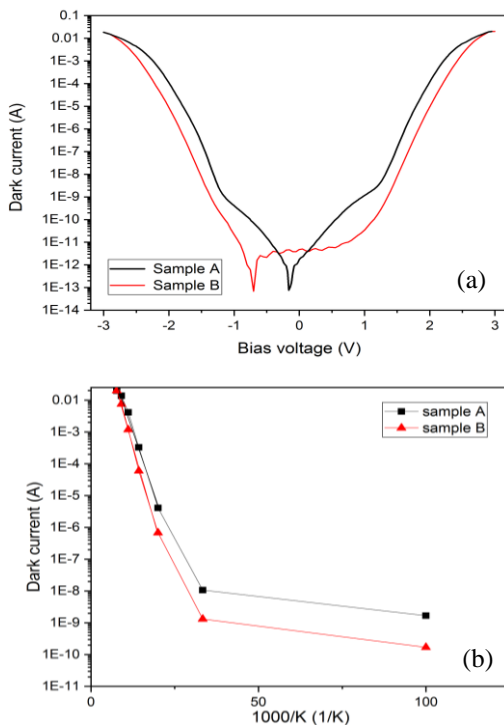


Fig. 4: (a) I-V curves in the dark (dark current) as a function of bias voltage for the two samples at 12K; (b) Arrhenius plot of the dark current of the two devices at a bias of -1.2V (where the detectivity is maximum).

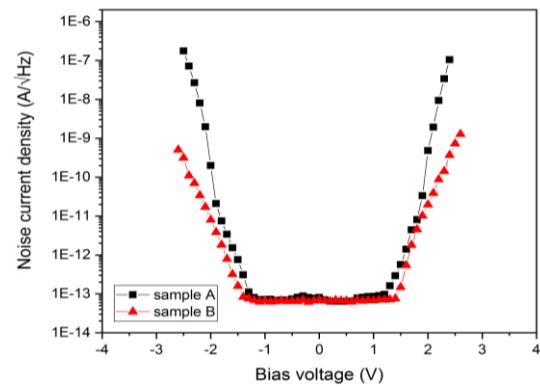


Fig. 5: Noise-current density in the dark as a function of bias voltage for the two samples at 12K.

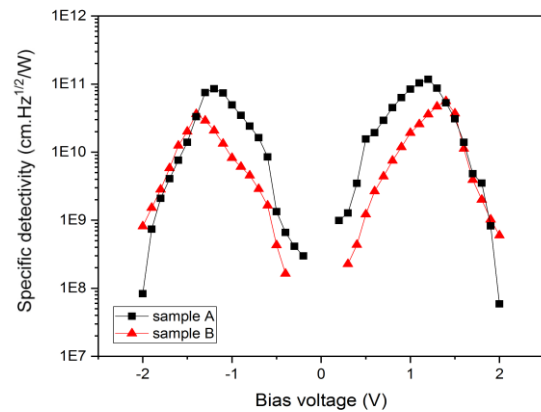


Fig. 6: Specific detectivity of the SML-QDIPs at 12K.

The noise current density ($i_n/\sqrt{\Delta f}$) in the dark is reported in Fig. 5 as a function of the bias voltage. It was obtained measuring the noise current i_n with a spectrum analyzer and normalizing its value with respect to the frequency range Δf used in the measurements. At low bias, the signal was constant, as the measurements were limited by the noise floor of the experimental setup. At high bias, the noise current density follows the same trends as the dark current curves, as expected. Indeed, in photoconductive photodetectors, Shot and Johnson noises are usually very small, and the main source of noise is due to the generation-recombination (g-r) noise of the dark current [20].

Fig. 6 shows the specific detectivity D^* of the devices that was calculated using the expression

$$D^* = \frac{R \sqrt{A \cdot \Delta f}}{i_n}$$

where R is the responsivity and A is the optical area of the detectors [21]. Although the responsivity curves are monotonic, the noise curves have a low-value plateau at low bias that leads to a maximum detectivity where the noise suddenly starts to increase. As a consequence, the maximum specific-detectivity values of $1.13 \times 10^{11} \text{ cm Hz}^{1/2} \text{ W}^{-1}$ and $5.6 \times 10^{10} \text{ cm Hz}^{1/2} \text{ W}^{-1}$ were achieved in sample A and sample B, respectively, and then the curves started to decrease abruptly at higher bias as a result of the much larger noise. Since both noise curves were very similar at low bias (Fig. 5), the difference in the maximum detectivity mainly comes from the higher responsivity of sample A.

So far, it seems that using an InAs coverage of 0.5 ML (sample A) is better than 0.35 ML (sample B). Although it is generally better to change a single parameter at a time to check its influence on the devices performance, in this specific case it might lead to erroneous conclusions, since the constant Si doping used in the present work was originally optimized for sample A but was probably not ideally suited for sample B, due to its higher density of SML-QDs. Therefore, a study varying the doping of the thin GaAs interlayer should also be performed in sample B in order to confirm that sample A is definitely superior.

Another point worth mentioning here is that most papers about SML-QDs report growth conditions similar to those of SK-QDs, which include a high As flux during InAs deposition. Photoluminescence (PL) [22] and cross-sectional scanning tunneling microscopy (X-STM) [9] measurements clearly showed that, in such conditions, there is a unity incorporation and strong segregation of the In atoms (they are all initially incorporated into the crystal and later are allowed to segregate). However, in the presence of the much lower As flux needed to stabilize the (2×4) reconstruction (as used here), In incorporation is no longer unity and In segregation is slightly enhanced, yielding layers with a lower In content. As a consequence, the 2D InAs islands are probably smaller and more easily dissolved, leading to SML-QDs looking like small In-rich InGaAs clusters embedded in a thick InGaAs layer having a lower In content [9]. Therefore, a more comprehensive investigation of the influence of the InAs coverage in the presence of a (2×4) surface reconstruction should also involve values of the InAs coverage larger than 0.5 ML that might eventually provide even higher detectivities than the one reported here for sample A.

IV. CONCLUSION

In conclusion, we investigated two SML-QDIPs grown in the presence of a (2×4) surface reconstruction and differing only by the InAs coverage during submonolayer deposition. Although SML-QDs formed with 0.5 ML of InAs provided the best results, optimization of the specific detectivity as a function of the InAs coverage is still inconclusive, as it should also involve an optimization of the Si doping—to deal with the different densities of SML-QDs—and should even consider larger InAs coverages (e.g., 0.6 and 0.7 ML) to compensate for the lower incorporation and stronger segregation of In atoms in the presence of a low As flux.

REFERENCES

- [1] P. Martyniuk and A. Rogalski, "Quantum-dot infrared photodetectors: Status and outlook", *progress in quantum electronics*, vol. 32, pp. 89–120, 2008.
- [2] J. D. Bimberg, M. Grundmann, and N. N. Ledentsov, *Quantum Dot Heterostructures*, Wiley, 1999.
- [3] V. Ryzhii, Khmyrova, M. Ryzhii, and V. Mitin, "Comparison of dark current, responsivity and detectivity in different intersubband infrared photodetectors", *semiconductor science and technology*, vol. 19, pp. 8–16, 2004.
- [4] F. Patella, M. Fanfoni, F. Arciprete, S. Nufri, E. Placidi, and A. Balzarotti, "Kinetic aspects of the morphology of self-assembled InAs quantum dots on GaAs(001)", *Applied Physics Letters*, vol. 78, pp. 320–322, 2001.
- [5] I. L. Krestnikov, N. N. Ledentsov, A. Hoffmann, and D. Bimberg, "Arrays of two-dimensional islands formed by submonolayer insertions: growth, properties, devices", *Physics Status Solidi A*, vol. 183, pp. 207–233, 2001.
- [6] Phu Lam, Jiang Wu, Mingchu Tang, Qi Jiang, Sabina Hatch, Richard Beanland, James Wilson, Rebecca Allison, Huiyun Liu "Submonolayer InGaAs/GaAs quantum dot solar cells", *Solar Energy Materials & Solar Cells*, vol. 126, pp. 83–87, 2014.
- [7] J. O. Kim, S. Sengupta, A. V. Barve, Y. D. Sharma, S. Adhikary, S. J. Lee, S. K. Noh, M. S. Allen, J. W. Allen, S. Chakrabarti, and S. Krishna, "Multi-stack InAs/InGaAs sub-monolayer quantum dots infrared photodetectors", *Applied Physics Letters*, vol. 102, pp. 011131(1–4), 2013.
- [8] David Z.-Y. Ting, Sumith V. Bandara, Sarath D. Gunapala, Jason M. Mumolo, Sam A. Keo, Cory J. Hill, John K. Liu, Edward R. Blazejewski, Sir B. Rafol, and Yia-Chung Chang, "Submonolayer quantum dot infrared photodetector", *Applied Physics Letters*, vol. 94, pp. 111107(1–3), 2009.
- [9] Gajjala R S R, Hendriks A L, Alzeidan A, Cantalice T F, Quivy A A and Koenraad P M, "Cross-sectional scanning tunneling microscopy of InAs/GaAs(001) submonolayer quantum dots", *Physical Review Materials*, vol. 4, pp. 114601(1–7), 2020.
- [10] S. Sengupta, J. O. Kim, A. V. Barve, S. Adhikary, Y. D. Sharma, N. Gautam, S. J. Lee, S. K. Noh, S. Chakrabarti and S. Krishna, "Submonolayer quantum dots in confinement enhanced dots-in-a-well heterostructure", *Applied Physics Letters*, vol. 100, pp. 191111(1–4), 2012.
- [11] Y. H. Kim, S. J. Kim, S. K. Noh, Jong S. Kim, and Jin S. Kim, "Evolutional Feature of InAs/GaAs Quantum Dots with Coverages from Submonolayer to a Few Monolayers", *Journal of the Korean Physical Society*, vol. 60, pp. 1785–1788, 2012.
- [12] A Alzeidan, T. F. de Cantalice, A. J. Garcia, C. F. Deneke, A. A. Quivy, "Investigation of the quantum confinement anisotropy in a submonolayer quantum dot infrared photodetector", 34th symposium on microelectronics technology and devices (SBMicro), pp. 1–4, 2019
- [13] J. G. Belk, C. F. McConville, J. L. Sudijono, T. S. Jones, and B. A. Joyce, "Surface alloying at InAs-GaAs interfaces grown on (001) surfaces by molecular beam epitaxy", *Surface Science*, vol. 387, pp. 213–226, 1997.
- [14] G. R. Bell, T. J. Krzyzewski, P. B. Joyce, and T. S. Jones, "Island size scaling for submonolayer growth of InAs on GaAs(001)- (2×4): strain and surface reconstruction effects", *Physical Review B*, vol. 61, pp. 551–554, 2000.
- [15] Cantalice T F, Alzeidan A, Urahata S M and Quivy A A, "In-situ measurement of Indium segregation in InAs/GaAs submonolayer quantum dots", *Materials Research Express*, vol. 6, pp. 126205 (1–6), 2019.
- [16] Saumya Sengupta, Arjun Mandal, Hemant Ghadi, Subhananda Chakrabarti, and Keshav Lal Mathur, "Comprehensive study on molecular beam epitaxy-grown InAs sub-monolayer quantum dots with different capping combinations", *Journal of Vacuum Science & Technology B, Nanotechnology and Microelectronics*, vol. 31, pp. 03C136 (1–4), 2013.
- [17] L. Yu, D. Jung, S. Law, J. Shen, J. J. Cha, M. L. Lee, and D. Wasserman, "Controlling quantum dot energies using submonolayer bandstructure engineering", *Applied Physics Letter*, vol. 105, pp. 081103(1–5), 2014.
- [18] V. P. LaBella, M. R. Krause, Z. Ding, and P. M. Thibado, "Arsenic-rich GaAs(0 0 1) surface structure", *Surface Science Reports*, vol. 60, pp. 1–53, 2005.
- [19] T. Asano, A. Madhukar, K. Mahalingam, and G. J. Brown, "Dark current and band profiles in low defect density thick multilayered GaAs/InAs self-assembled quantum dot structures for infrared detectors", *Journal of Applied Physics*, vol. 104, pp. 113115(1–5), (2008).
- [20] F.N. Hooge. "1/f noise sources", *IEEE Trans. Electron Devices*, vol. 41(11), pp. 1926–1935, 1994.
- [21] J. D. Vincent, *Fundamentals of Infrared Detector Operation and Testing*, Wiley, 1990.
- [22] K. Muraki, S. Fukatsu, Y. Shiraki, and R. Ito, "Surface segregation of In atoms during molecular beam epitaxy and its influence on the energy levels in InGaAs/GaAs quantum wells", *Applied Physics Letters*, vol. 61, pp. 557–559, 1992.